BJR https://doi.org/10.1259/bjr.20170443

Received: 12 June 2017 | Revised: 25 April 2018 | Accepted: 09 May 2018

Cite this article as:
Gariani J, Martin SP, Botsikas D, Becker CD, Montet X. Evaluating the effect of increased pitch, iterative reconstruction and dual source CT on dose reduction and image quality. *Br J Radiol* 2018; **91**: 20170443.

FULL PAPER

Evaluating the effect of increased pitch, iterative reconstruction and dual source CT on dose reduction and image quality

JOANNA GARIANI, MD, STEVE P MARTIN, MD, DIOMIDIS BOTSIKAS, MD, CHRISTOPH D BECKER, MD and XAVIER MONTET, MD

Division of Radiology, Department of Imaging and Medical Information Sciences, Geneva University Hospitals, Geneva, Switzerland

Address correspondence to: Dr Joanna Gariani
E-mail: *joanna.gariani@hcuge.ch*

Objective: To compare radiation dose and image quality of thoracoabdominal scans obtained with a high-pitch protocol (pitch 3.2) and iterative reconstruction (Sinogram Affirmed Iterative Reconstruction) in comparison to standard pitch reconstructed with filtered back projection (FBP) using dual source CT.
Methods: 114 CT scans (Somatom Definition Flash, Siemens Healthineers, Erlangen, Germany), 39 thoracic scans, 54 thoracoabdominal scans and 21 abdominal scans were performed. Analysis of three protocols was undertaken; pitch of 1 reconstructed with FBP, pitch of 3.2 reconstructed with SAFIRE, pitch of 3.2 with stellar detectors reconstructed with SAFIRE. Objective and subjective image analysis were performed. Dose differences of the protocols used were compared.
Results: Dose was reduced when comparing scans with a pitch of 1 reconstructed with FBP to high-pitch scans with a pitch of 3.2 reconstructed with SAFIRE with a reduction of volume CT dose index of 75% for thoracic scans, 64% for thoracoabdominal scans and 67% for abdominal scans. There was a further reduction after the implementation of stellar detectors reflected in a reduction of 36% of the dose–length product for thoracic scans. This was not at the detriment of image quality, contrast-to-noise ratio, signal-to-noise ratio and the qualitative image analysis revealed a superior image quality in the high-pitch protocols.
Conclusion: The combination of a high pitch protocol with iterative reconstruction allows significant dose reduction in routine chest and abdominal scans whilst maintaining or improving diagnostic image quality, with a further reduction in thoracic scans with stellar detectors.
Advances in knowledge: High pitch imaging with iterative reconstruction is a tool that can be used to reduce dose without sacrificing image quality.

INTRODUCTION

The number of CT examinations continues to rise and is currently responsible for around 70% of medical radiation exposures.[1–5] Concerns exist that the radiation exposure from CT scanning contributes to an increasing number of radiation-induced cancers.[6] It is, therefore, necessary to reduce the radiation exposure of each CT scan by adopting the as low as reasonably achievable principle whilst ensuring diagnostic quality.[7] Different techniques exist to limit the radiation exposure of CT. Tube current and tube voltage reduction, automated tube current modulation, noise reduction filters, optimization of CT hardware such as detectors and more recently the use of iterative reconstruction (IR) algorithms are amongst the different strategies available for dose reduction.[8–13]

Second-generation dual source CT (DSCT) with 128-slice detectors now also enables scanning at a high-pitch. DSCT systems have two sets of X-ray tube-detector pairs with the two acquisition systems mounted at an angular offset of 90° on the rotating gantry. Each detector acquires 64 overlapping slices per rotation. DSCT allows spiral acquisition for pitch values higher than 3 without image distortion, this is because the presence of two detector banks provides volume coverage without gaps at high pitch values.[14] Studies have shown that high-pitch CT is beneficial not only for cardiac imaging but also in routine chest and abdominal CT by decreasing radiation dose whilst maintaining diagnostic image quality.[15–17]

A conventional CT detector consists of a scintillator, a photodiode, and a circuit board with an analogue-to-digital converter (ADC) in separate components, the signal is affected by resistance and capacitative loss as it travels through the components. Integrated detectors integrate the

ADC chip directly with the photodiode to directly generate the signal and reduce electronic noise.[18]

The purpose of this study was to evaluate image quality of high-pitch CT for chest and abdominal scans, taking into account two major technological breakthroughs. The first one was the introduction of DSCT allowing high-pitch imaging. The second one was the introduction of new integrated CT detectors. Our hypothesis is that image quality will improve with this new technology.

METHODS AND MATERIALS

Patients

The study was approved by the ethics committee of Geneva University Hospital. The total study sample of 114 contrast-enhanced CT scans acquired on a SOMATOM Definition Flash unit (Siemens Healthcare GmbH, Erlangen, Germany) that was later upgraded to integrated CT detectors consisted of 3 groups of 38 patients. The differences in age, gender, body mass index and CT examinations (chest CT $n = 13$; thoracoabdominal CT $n = 18$; CT abdominal $n = 7$) between the three groups were not significant. Group 1 corresponded to a standard-pitch CT (pitch 0.6) reconstructed with filtered back projection (FBP), acquired with conventional CT detectors (Ultra Fast Ceramics, UFC, Siemens Healthcare, Forchheim, Germany). Group 2 corresponded to a high-pitch protocol reconstructed with Sinogram Affirmed Iterative Reconstruction (SAFIRE), acquired with conventional CT detectors (UFC detectors). Group 3 corresponded to a high-pitch protocol reconstructed with SAFIRE and acquired with integrated CT detectors (Stellar detectors, Siemens Healthcare, Forchheim, Germany). The clinical reasons for performing the CT studies were as follows; neoplasia ($n = 77$), infection ($n = 20$), digestive pathology ($n = 11$), other ($n = 6$).

The decision whether high-pitch CT was performed was made by the radiologist supervising the examination. Only patients covered by the 33 cm scan field of view were included as this was the maximum field of view available for high-pitch dual source scanning. The anatomical coverage of the chest scans was from the lung apices to lung bases, for the abdominal scans from the lung bases to the pubic symphysis and the throacoabdominal scans from the lung apices to the pubic symphysis. Parameters of patient demographics are summarized in Table 1. Scan acquisition and reconstruction parameters are detailed in Table 2. Iodinated contrast media were intravenously injected with the following protocols, for thoracic imaging : 0.3 mg iodine per kg of iohexol (Iohexol, Accupaque 350®, 350 mg of iodine ml^{-1}, GE Healthcare, Milwaukee, WI) were injected in an antecubital vein at a flow rate of 3 ml s^{-1}, followed by 20 ml saline flush at a flow rate of 3 ml s^{-1}. The acquisition started 35 s after the beginning of the injection. For abdominal and thoracoabdominal imaging : 0.6 mg iodine per kg of Iohexol (Iohexol, Accupaque 350®, 350 mg of iodine ml^{-1}, GE Healthcare, Milwaukee, WI) were injected in a antecubital vein at a flow rate of 3 ml s^{-1}, followed by 30 ml saline flush at a flow rate of 3 ml s^{-1}. The acquisition started 65 s after the beginning of the injection.

To take into account small morphological differences between the different groups, we have used size specific dose estimate as given in the AAPM report 204.[19] The size specific dose estimate is defined as the dose–length product (DLP) multiplied by a correction factor and takes into account the diameter of the patient. For the thoracic and thoracoabdominal scans, the lateral diameter was measured at the level of the carina, perpendicular to the *z*-axis. For the abdominal scans, the lateral diameter was measured at the height of the iliac crest, perpendicular to the *z*-axis. The volume CT dose index (CTDIvol) and DLP were retrieved from the dose report generated by the scanner.

Quantitative image analysis

Axial images were reconstructed at 2 mm slice thickness using a soft tissue kernel. Regions of interest (ROIs) were drawn by Radiologist 1 using the image processing software OsiriX MD (Pixmeo, Switzerland) in the scapula muscle, thyroid gland, trachea, aorta, main pulmonary artery, right and left ventricle, myocardium, hepatic veins, portal vein, right and left portal branches, hepatic parenchyma, pancreatic parenchyma, splenic parenchyma, renal cortex, renal medulla, adrenal gland, psoas muscle, bladder contents, intra-abdominal fat. The ROIs were sized to cover the largest surface of each anatomical structure. There were no significant differences in Hounsfield units (HUs) of the different ROIs for the three scanning protocols. The mean HU of the myocardium and left ventricle were used to calculate the contrast-to-noise ratio (CNR) on chest scans and the mean HU values of the portal vein and hepatic parenchyma were used to calculate the CNR of the abdominal scans [CNR = (HU_1–HU_2)/standard deviation of HU_2]. Signal-to-noise ratio (SNR) was calculated using a round ROI of 1 cm^2 placed in the myocardium and the liver parenchyma (SNR = HU organ/standard deviation HU organ).

Qualitative image analysis

Each scan was evaluated independently by two radiologists (Radiologist 1 with 7 years and Radiologist 2 with 8 years of experience in body imaging). Images were anonymized with removal of all annotations relating to scan protocol and organized randomly. Overall image quality was assessed using a

Table 1. Patient demographics

	Low pitch, FBP	High pitch, SAFIRE	High pitch, SAFIRE, Stellar	
Mean age ± SD (years)	65 ± 2	66 ± 3	64 ± 3	$p = 0.80$
Number of male/female	24/14	21/17	21/17	$p = 0.75$
Mean BMI (range) (kg m^{-2})	24.82 (14.96–37.74)	22.86 (16.49–29.67)	25.44 (17.37–38.06)	$p = 0.09$
Pitch	0.6	3.2	3.2	NA

BMI, body mass index; FBP, filtered back projection; SAFIRE, Sinogram Affirmed Iterative Reconstruction; SD, standard deviation.
There was no statistically significant difference in age, sex, or BMI amongst groups.

Table 2. Acquisition and scan parameters

	Acquisition parameters								Reconstruction parameters		
	Collimation (mm)	Pitch	Rotation time (s)	Detector type	Tube A		Tube B		Algorithm	Kernel	Slice thickness—interval (mm)
					kV	mAs ref	kV	mAs ref			
Group 1	64 × 2×0.6	0.6	0.7	Conventional	100	250	140	193	FBP	b30	2–1
Group 2	64 × 2×0.6	3.2	0.28	Conventional	120	140–190	120	140–190	SAFIRE 3	i31	2–1
Group 3	64 × 2×0.6	3.2	0.28	Stellar	120	110–190	120	110–190	SAFIRE 3	i31	2–1

FBP, filtered back projection; SAFIRE, Sinogram Affirmed Iterative Reconstruction

Table 3. Dose estimates

	DLP (mGycm)		CTDIvol (mGy)		SSDE (mGy)	
Thorax	Mean ± SEM	*p*-values	Mean ± SEM	*p*-values	Mean ± SEM	*p*-values
Low pitch, FBP	313.90 ± 30.41		21.85 ± 1.56		11.67 ± 1.05	
High pitch, SAFIRE	216.30 ± 18.14	$p = 0.078$	5.45 ± 0.50	$p < 0.0001$	2.78 ± 0.15	$p = 0.014$
High pitch, Stellar, SAFIRE	125.50 ± 8.76	$p = 0.009$	3.49 ± 0.35	$p = 0.295$	1.35 ± 0.05	$p = 0.005$
Thoracoabdominal						
Low pitch, FBP	767.90 ± 60.22		25.73 ± 1.83		14.75 ± 0.93	
High pitch, SAFIRE	416.50 ± 33.59	$p < 0.0001$	9.14 ± 1.57	$p < 0.0001$	5.28 ± 0.90	$p < 0.0001$
High pitch, Stellar, SAFIRE	438.60 ± 33.68	$p > 0.999$	8.93 ± 1.37	$p > 0.999$	4.11 ± 0.60	$p = 0.263$
Abdominal						
Low pitch, FBP	831.40 ± 88.84		16.61 ± 1.43		8.41 ± 0.35	
High pitch, SAFIRE	249.40 ± 29.65	$p = 0.001$	5.46 ± 0.44	$p = 0.004$	3.62 ± 0.23	$p = 0.040$
High pitch, Stellar, SAFIRE	290.70 ± 30.02	$p > 0.999$	5.30 ± 0.53	$p > 0.999$	2.90 ± 0.14	$p = 0.186$

CTDIvol, Computed Tomography dose index volume; DLP, dose–length product; FBP, filtered back projection; SAFIRE, Sinogram Affirmed Iterative Reconstruction; SEM, standard error of the mean; SSDE, sized-specific dose estimate.

Figure 1. CNR left ventricle-myocardium. CNR (± SEM) was significantly higher when comparing the low-pitch scans reconstructed with FBP to both the high-pitch scans with SAFIRE and the high-pitch scans with SAFIRE and stellar detectors (3.29 ± 0.37 *vs* 5.67 ± 0.83, p = 0.03 and 3.29 ± 0.37 *vs* 5.69 ± 0.87, p = 0.03 respectively). CNR, contrast-to-noise ratio; FBP, filtered back projection; SAFIRE, Sinogram Affirmed Iterative Reconstruction; SEM, standard error of the mean.

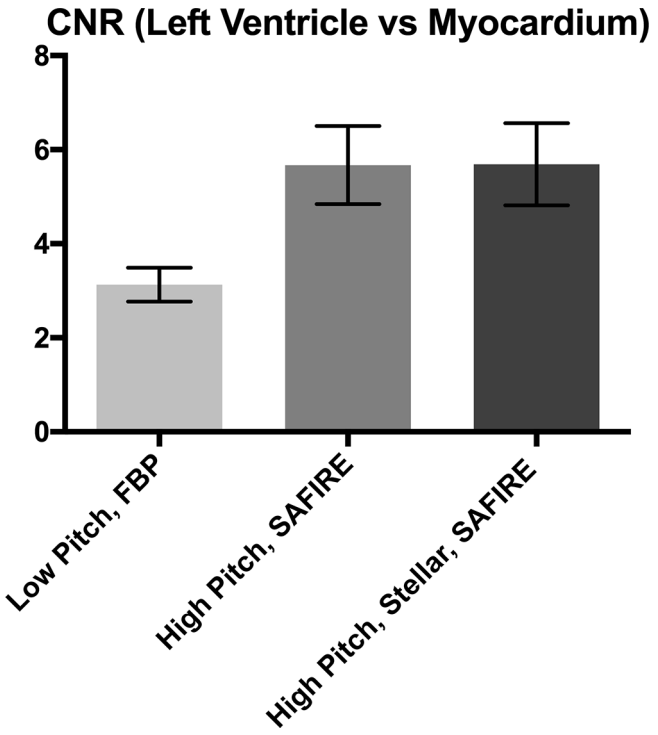

Figure 2. CNR portal vein–liver parenchyma. The abdominal scans showed no differences in CNR (± SEM) despite the significant dose reduction in both the high-pitch SAFIRE scans and high pitch, SAFIRE and stellar detector scans. The low-pitch FBP protocol compared to the high pitch, SAFIRE (3.997 ± 0.4629 *vs* 2.932 ± 0.3513, p = 0.5898) and the low-pitch FBP compared to high pitch, SAFIRE and stellar detectors (3.997 ± 0.4629 *vs* 3.349 ± 0.37, p > 0.99). CNR, contrast-to-noise ratio; FBP, filtered back projection; SAFIRE, Sinogram Affirmed Iterative Reconstruction; SEM, standard error of the mean.

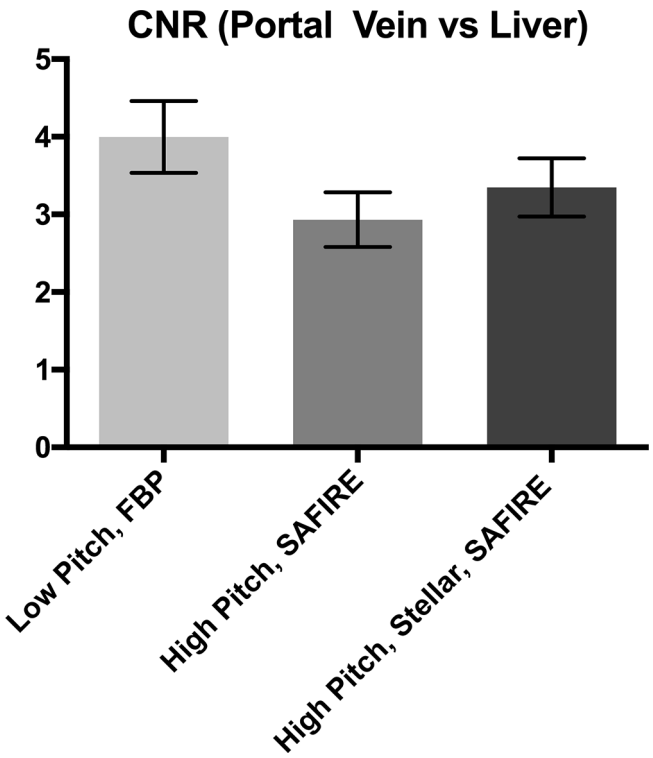

5-point Likert scale; 1 = bad, not diagnostic, 2 = poor, diagnostic confidence substantially reduced, 3 = moderate, sufficient for diagnosis, 4 = good, 5 = excellent.

Lesion/organ conspicuity was assessed using a 5-point Likert scale; 1 = very poor, almost not visible; 2 = poor; 3 = intermediate; 4 = good 5 = excellent.

Each scan was then analyzed for motion artifacts on a 5-point Likert scale; 1 = major, unacceptable; 2 = substantial, above average; 3 = moderate, average; 4 = minor, below average; 5 = absent.

10 cases that were not included in the study were analyzed by the readers by consensus to train readers on the different scales.

Statistical analysis

Statistical analysis was performed with Prism (Prism, v. 6b, 2012, Graphpad Software, San Diego, CA). For continuous values, the results are presented as mean ± standard error of the mean. For discrete values, the results are presented as 95% confident intervals.

Non-normally distributed data sets (established from Kolmogorov–Smirnov tests) were compared using Kruskall–Wallis test with Dunn *post-hoc* test. Normally distributed data sets were compared using ANOVA test with Bonferroni *post-hoc* test. Two-sided testing was used. Differences were considered significant at $p < 0.05$.

RESULTS

Dose estimates

Implementation of a high-pitch protocol with IR allowed a reduction in dose in thoracic scans with a further reduction observed after the introduction of stellar detectors. Radiation dose was reduced in thoracoabdominal scans when comparing a low-pitch FBP protocol with a high-pitch IR protocol. This reduction in dose remained unchanged after the introduction of stellar detectors. Similar results were found in abdominal scans with a significant reduction in dose when comparing the low-pitch FBP protocol with a high-pitch IR protocol and no significant reduction after the introduction of stellar detectors. The displayed CTDIvol was comparable to that measured as part of the routine biannual controls of delivered CTDIvol with a tolerance of 10% difference between displayed and delivered CTDIvol in compliance with national legislation.

These results are summarized in Table 3.

Figure 3. SNR myocardium. SNR (± SEM) was similar for the three groups (low-pitch FBP = 5.667 ± 0.42, high-pitch SAFIRE 5.48 ± 0.35, high-pitch SAFIRE and stellar detectors 6.64 ± 0.51, $p \geq 0.27$). FBP, filtered back projection; SAFIRE, Sinogram Affirmed Iterative Reconstruction; SEM, standard error of the mean; SNR, signal-to-noise ratio.

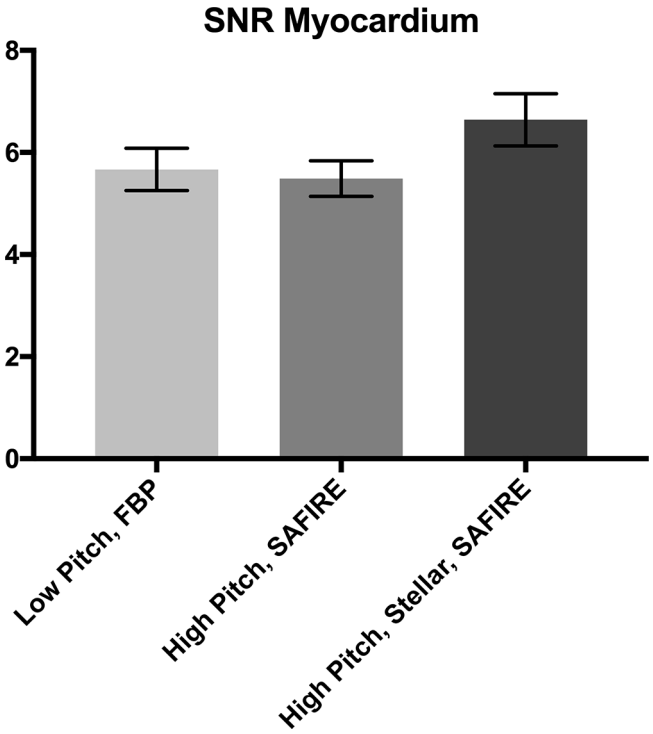

Figure 4. SNR liver. SNR (± SEM) was similar for the three groups liver (low-pitch FBP = 6.08 ± 0.44, high-pitch SAFIRE 5.18 ± 0.30, high-pitch SAFIRE and stellar detectors 5.67 ± 0.34, $p > 0.14$). CNR, contrast-to-noiseratio; FBP, filtered back projection; SAFIRE, Sinogram Affirmed Iterative Reconstruction; SEM, standard error of the mean.

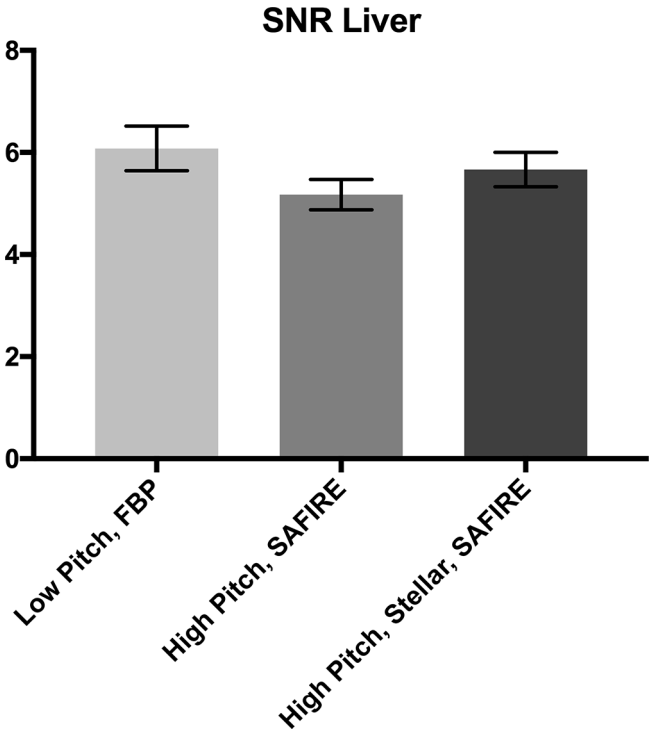

Quantitative image analysis

The thoracic scans had a better CNR despite the significant X-ray dose reduction when comparing the low pitch, FBP protocol to both the high pitch, SAFIRE protocol (3.29 ± 0.37 vs 5.67 ± 0.83, $p = 0.03$) and the high pitch, SAFIRE, stellar detector protocol (3.29 ± 0.37 *vs* 5.69 ± 0.87, $p = 0.03$) (Figure 1).

The abdominal scans had similar CNR when comparing the three different protocols despite the significant decrease in dose that resulted from the introduction of a high-pitch protocol. The low-pitch FBP compared to high pitch, SAFIRE (3.997 ± 0.4629 *vs* 2.932 ± 0.3513, $p = 0.5898$) and low-pitch FBP compared to high pitch, SAFIRE and stellar detectors (3.997 ± 0.4629 *vs* 3.349 ± 0.37, $p > 0.99$) (Figure 2).

SNR was similar for the three groups at the level of the myocardium (low-pitch FBP = 5.667±0.42, high-pitch SAFIRE 5.48 ± 0.35, high-pitch SAFIRE and stellar detectors 6.64 ± 0.51, $p \geq 0.27$) (Figure 3) and at the level of the liver (low-pitch FBP = 6.08 ± 0.44, high-pitch SAFIRE 5.18 ± 0.30, high-pitch SAFIRE and stellar detectors 5.67 ± 0.34, $p > 0.14$.) (Figure 4).

Qualitative image analysis

Table 4 summarizes the results of qualitative image analysis. Overall image quality was comparable for the low-pitch FBP and high-pitch SAFIRE protocols, with scores ranging from 4.05 to 4.15 and 3.99–4.10 respectively, considered as good with no statistically significant difference between the groups. There was a statistically significant improvement in subjective image quality after the introduction of stellar detectors with scores ranging from 4.28 to 4.37.

Motion artifacts were considered as moderate for the low-pitch FBP scans, with scores ranging from 3.33–3.48. The

Table 4. Subjective image quality

	Low pitch, FBP	High pitch, SAFIRE	*p*	High pitch, SAFIRE, Stellar	*p*
Image quality (95% CI)	4.05–4.15	3.99–4.10	NS	4.28–4.37	<0.0001
Motion artifacts (95% CI)	3.33–3.48	4.03–4.21	<0.0001	4.12–4.29	<0.0001

CI, confidence interval; FBP, filtered back projection; SAFIRE, Sinogram Affirmed Iterative Reconstruction.
There was a significant improvement in image quality when comparing the low- pitch scans with FBP to the high-pitch scans with SAFIRE and stellar detectors but no difference between the low-pitch FBP scans and the high-pitch SAFIRE scans. There was a statistically significant improvement of motion artifacts when comparing the low-pitch FBP scans to both the high-pitch SAFIRE scans and the high pitch, SAFIRE, stellar detect scans.

Figure 5. Thoracoabdominal scans in the coronal plane with soft-tissue window setting of the protocols used illustrating a decrease in radiation dose in the high-pitch protocols without sacrificing image quality. BMI, body mass index; CTDIvol, Computed Tomography dose index volume; DLP, dose–length product; FBP, filtered back projection; SAFIRE, Sinogram Affirmed Iterative Reconstruction; SEM, standarderror of the mean; SSDE, sized-specific dose estimate.

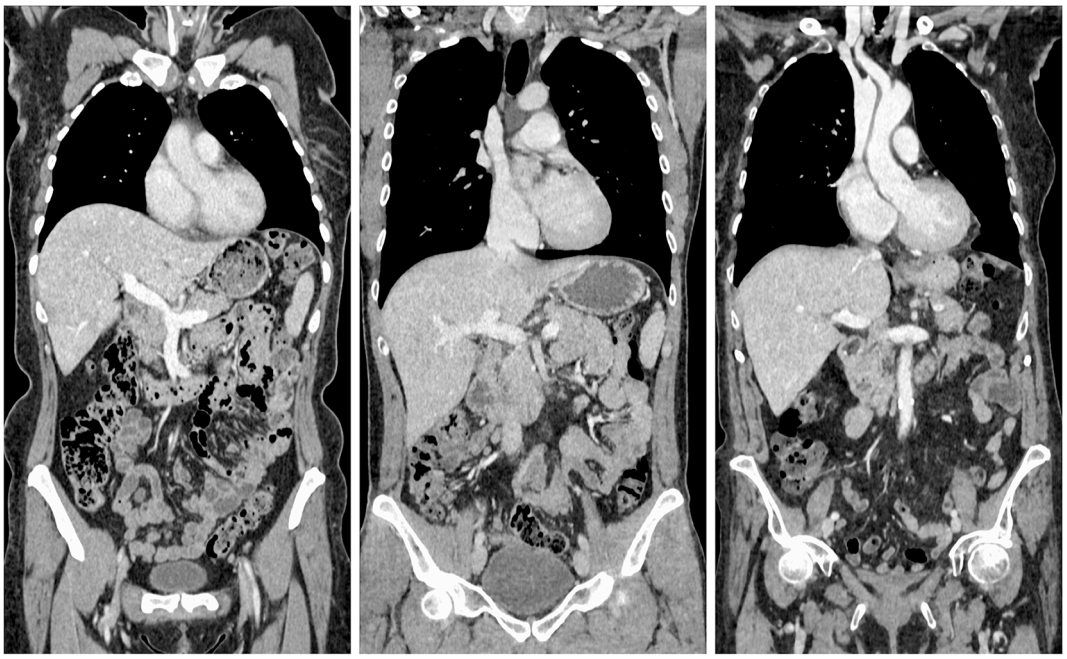

FBP UFC detectors Pitch 0.6		SAFIRE UFC detectors Pitch 3.2		SAFIRE Stellar detectors Pitch 3.2	
BMI (m/kg^2)	25.74	BMI (m/kg^2)	25.47	BMI (m/kg^2)	27.18
CTDIvol (mGy)	29	CTDIvol (mGy)	5.82	CTDIvol (mGy)	4.66
DLP (mGy-cm)	863	DLP (mGy-cm)	394	DLP (mGy-cm)	310
SSDE (mGy)	15.95	SSDE (mGy)	3.09	SSDE (mGy)	2.56

implementation of a high-pitch protocol with SAFIRE resulted in a significant decrease in motion artifacts and a further decrease with stellar detectors, both statistically significant with scores ranging from 4.03 to 4.21 and 4.12–4.29 respectively (Figures 5–6).

Figure 6. Thoracic scans in the axial plane with soft-tissue window setting. The low-pitch protocol shows significant motion artifacts of the aortic root and the ostium of the left coronary artery is not identifiable (asterisk). With the introduction of a high-pitch protocol, there is a significant decrease in motion artifacts allowing not only the visualization of the aortic valve leaflets (black arrows) but also the ostium of the right coronary artery (dotted arrow). BMI, body mass index; CTDIvol, Computed Tomography dose index volume; DLP, dose–length product; FBP, filtered back projection; SAFIRE, Sinogram Affirmed Iterative Reconstruction; SEM, standard error of the mean; SSDE, sized-specific dose estimate.

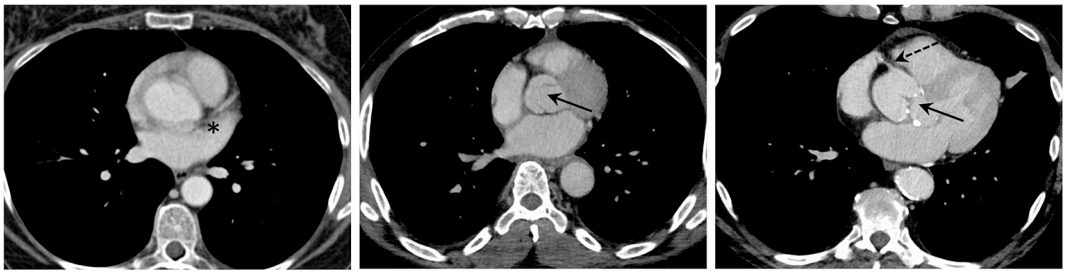

FBP UFC detectors Pitch 0.6		SAFIRE UFC detectors Pitch 3.2		SAFIRE Stellar detectors Pitch 3.2	
BMI (m/kg^2)	25.78	BMI (m/kg^2)	24.97	BMI (m/kg^2)	24.06
CTDIvol (mGy)	24.4	CTDIvol (mGy)	6.54	CTDIvol (mGy)	5.76
DLP (mGy-cm)	687	DLP (mGy-cm)	477	DLP (mGy-cm)	412
SSDE (mGy)	13.42	SSDE (mGy)	3.34	SSDE (mGy)	2.94

Kendall's coefficient of concordance amongst the readers was of 0.787 for both image quality and motion artifacts.

DISCUSSION

The widespread use of CT examinations as a robust and efficient diagnostic tool for both the chest and abdomen have led to the development of different dose reduction techniques. FBP as a reconstruction algorithm allows rapid image reconstruction but suffers from various limitations due to the approximation of the real focal spot and detector sizes and the corruption of data by quantum and electronic noise during acquisition.[20] The introduction of IR techniques, such as SAFIRE, more accurately match the reconstructed image with the acquired projection data thus leading to a significant reduction in noise.[21] This ultimately renders this type of reconstruction algorithm a powerful tool in dose reduction. Another technique that is available to reduce dose is to increase pitch. The second-generation dual source CT scanner with 128-slice detectors enables scanning with a pitch of up to 3.2 for the chest and abdomen, translating to a table feed of up to 46 cm s^{-1}.

Our study showed that a significant dose reduction was possible when combining these techniques and comparing a low-pitch protocol reconstructed with FBP with a high-pitch protocol reconstructed with an IR algorithm, SAFIRE. This dose was further decreased for thoracic scans with the implementation of integrated CT detectors (Stellar detectors). These detectors directly coupled the photodiode with the ADC, reducing the electronic noise and hence increasing the CNR.[22] This illustrates that the combination of technical advances allows dose reduction in a routine clinical setting. This dose reduction was not at the cost of image quality as CNR was superior in the high-pitch protocols reconstructed with SAFIRE for the thoracic scans and remained stable in abdominal and thoracoabdominal scans despite a significant reduction in dose. This was also reflected in the subjective analysis as overall image quality was deemed highest with the high pitch, SAFIRE, and stellar detector protocol.

Previous studies have shown a dose reduction ranging from 40 to 60% when implementing IR in comparison to FBP in thoracic, thoracoabdominal and abdominal scans.[23–25] When implementing a high-pitch scanning protocol in chest and abdominal scan Amacker et al showed a dose reduction of 26 and 48% respectively.[17] Our study showed a dose reduction that was superior and may be explained by the implementation of multiple dose reduction techniques; IR, high pitch, and integrated detectors.

Aside from the important dose reduction that was possible by the implementation of a high-pitch protocol, our study showed that there was a significant reduction in motion artifacts when comparing the low pitch, FBP protocol to both high-pitch SAFIRE protocols used. This has been illustrated by other groups particular for cardiac scans, in the pediatric population and in trauma patients.[26–30] Although both differences in CNR values and subjective image quality assessments were noted the clinical significance may vary. The reduction in motion artifacts as reflected by the improvement in qualitative analysis is more readily appreciated in practice than variations in CNR.

There is less available data on the effect of a high-pitch protocol on motion artifacts in routine thoracoabdominal scans. Our study showed a significant reduction in motion artifacts when using a high-pitch compared to standard-pitch protocol.

Differences have been described in the subjective appearance between IRs and FBP, with the prior being described as resulting in a waxy or plastic appearance of images.[31] In the objective analysis of our study, we did not find that this limited image quality.

Study limitations

The retrospective study design is a limitation of our study. Another limitation is that the first group of scans at low pitch with FBP was compared to a high-pitch protocol with SAFIRE. This was done to optimize the scan protocol and use all available technology but the drawback is a simultaneous modification of two different parameters. These modifications reflect the development of different technologies that were made available in our department. Another limitation is that only CNR was used, as a quantitative analysis tool of image quality, there are now other metrics that could be considered such as texture analysis. Image quality assessment was based on a limited number of parameters and this did not include spatial resolution and low contrast detectability. The population size was limited by the number of scans available in the high-pitch SAFIRE group before the installation of integrated detectors.

CONCLUSION

The combination of a high-pitch protocol with IR allows significant dose reduction in routine chest and abdominal scans whilst maintaining or improving diagnostic image quality, with a further reduction in thoracic scans with stellar detectors.

REFERENCES

1. Brenner DJ, Hall EJ. Computed tomography--an increasing source of radiation exposure. *N Engl J Med* 2007; **357**: 2277–84. doi: https://doi.org/10.1056/NEJMra072149
2. Martin DR, Semelka RC. Health effects of ionising radiation from diagnostic CT. *Lancet* 2006; **367**: 1712–4. doi: https://doi.org/10.1016/S0140-6736(06)68748-5
3. Smith-Bindman R, Lipson J, Marcus R, Kim KP, Mahesh M, Gould R, et al. Radiation dose associated with common computed tomography examinations and the associated lifetime attributable risk of cancer. *Arch Intern Med* 2009; **169**: 2078–86. doi: https://doi.org/10.1001/archinternmed.2009.427
4. Meer AB, Basu PA, Baker LC, Atlas SW. Exposure to ionizing radiation and estimate of secondary cancers in the era of high-speed CT scanning: projections from the Medicare population. *J Am Coll Radiol* 2012; **9**: 245–50.

doi: https://doi.org/10.1016/j.jacr.2011.12.007
5. Lin EC. Radiation risk from medical imaging. *Mayo Clin Proc* 2010; **85**: 1142–6. doi: https://doi.org/10.4065/mcp.2010.0260
6. Brenner DJ, Elliston CD. Estimated radiation risks potentially associated with full-body CT screening. *Radiology* 2004; **232**: 735–8. doi: https://doi.org/10.1148/radiol.2323031095
7. Bevelacqua JJ. Practical and effective ALARA. *Health Phys* 2010; **98**(Suppl 2): S39–S47. doi: https://doi.org/10.1097/HP.0b013e3181d18d63
8. Lee S, Yoon SW, Yoo SM, Ji YG, Kim KA, Kim SH, et al. Comparison of image quality and radiation dose between combined automatic tube current modulation and fixed tube current technique in CT of abdomen and pelvis. *Acta Radiol* 2011; **52**: 1101–6. doi: https://doi.org/10.1258/ar.2011.100295
9. Gies M, Kalender WA, Wolf H, Suess C. Dose reduction in CT by anatomically adapted tube current modulation. I. Simulation studies. *Med Phys* 1999; **26**: 2235–47. doi: https://doi.org/10.1118/1.598779
10. Kalra MK, Wittram C, Maher MM, Sharma A, Avinash GB, Karau K, et al. Can noise reduction filters improve low-radiation-dose chest CT images? Pilot study. *Radiology* 2003; **228**: 257–64. doi: https://doi.org/10.1148/radiol.2281020606
11. Pontana F, Duhamel A, Pagniez J, Flohr T, Faivre JB, Hachulla AL, et al. Chest computed tomography using iterative reconstruction vs filtered back projection (Part 2): image quality of low-dose CT examinations in 80 patients. *Eur Radiol* 2011; **21**: 636–43. doi: https://doi.org/10.1007/s00330-010-1991-4
12. Montet X, Hachulla AL, Neroladaki A, Lador F, Rochat T, Botsikas D, et al. Image quality of low mA CT pulmonary angiography reconstructed with model based iterative reconstruction versus standard CT pulmonary angiography reconstructed with filtered back projection: an equivalency trial. *Eur Radiol* 2015; **25**: 1665–71. doi: https://doi.org/10.1007/s00330-014-3563-5
13. Neroladaki A, Botsikas D, Boudabbous S, Becker CD, Montet X. Computed tomography of the chest with model-based iterative reconstruction using a radiation exposure similar to chest X-ray examination: preliminary observations. *Eur Radiol* 2013; **23**: 360–6. doi: https://doi.org/10.1007/s00330-012-2627-7
14. Petersilka M, Bruder H, Krauss B, Stierstorfer K, Flohr TG. Technical principles of dual source CT. *Eur J Radiol* 2008; **68**: 362–8. doi: https://doi.org/10.1016/j.ejrad.2008.08.013
15. Leschka S, Stolzmann P, Desbiolles L, Baumueller S, Goetti R, Schertler T, et al. Diagnostic accuracy of high-pitch dual-source CT for the assessment of coronary stenoses: first experience. *Eur Radiol* 2009; **19**: 2896–903. doi: https://doi.org/10.1007/s00330-009-1618-9
16. Alkadhi H, Stolzmann P, Desbiolles L, Baumueller S, Goetti R, Plass A, et al. Low-dose, 128-slice, dual-source CT coronary angiography: accuracy and radiation dose of the high-pitch and the step-and-shoot mode. *Heart* 2010; **96**: 933–8. doi: https://doi.org/10.1136/hrt.2009.189100
17. Amacker NA, Mader C, Alkadhi H, Leschka S, Frauenfelder T. Routine chest and abdominal high-pitch CT: an alternative low dose protocol with preserved image quality. *Eur J Radiol* 2012; **81**: e392–e397. doi: https://doi.org/10.1016/j.ejrad.2011.12.017
18. Ebner L, Knobloch F, Huber A, Landau J, Ott D, Heverhagen JT, et al. Feasible dose reduction in routine chest computed tomography maintaining constant image quality using the last three scanner generations: from filtered back projection to sinogram-affirmed iterative reconstruction and impact of the novel fully integrated detector design minimizing electronic noise. *J Clin Imaging Sci* 2014; **4**: 38. doi: https://doi.org/10.4103/2156-7514.137826
19. Boone JM, Strauss KJ, Cody DD, McCollough CH, McNitt-Gray MF, Thot TL. Comprehensive methodology for the evaluation of radiation dose in X-Ray computed tomography. 2011. Available from: https://www.aapm.org/pubs/reports/RPT_204.pdf.
20. Pan X, Sidky EY, Vannier M. Why do commercial CT scanners still employ traditional. *filtered back-projection for image reconstruction? Inverse Probl* 2009; **25**: 1230009.
21. Katsura M, Matsuda I, Akahane M, Sato J, Akai H, Yasaka K, et al. Model-based iterative reconstruction technique for radiation dose reduction in chest CT: comparison with the adaptive statistical iterative reconstruction technique. *Eur Radiol* 2012; **22**: 1613–23. doi: https://doi.org/10.1007/s00330-012-2452-z
22. Duan X, Wang J, Leng S, Schmidt B, Allmendinger T, Grant K, et al. Electronic noise in CT detectors: impact on image noise and artifacts. *AJR Am J Roentgenol* 2013; **201**: W626–W632. doi: https://doi.org/10.2214/AJR.12.10234
23. Morimoto LN, Kamaya A, Boulay-Coletta I, Fleischmann D, Molvin L, Tian L, et al. Reduced dose CT with model-based iterative reconstruction compared to standard dose CT of the chest, abdomen, and pelvis in oncology patients: intra-individual comparison study on image quality and lesion conspicuity. *Abdom Radiol* 2017; **42**: 2279–88. doi: https://doi.org/10.1007/s00261-017-1140-5
24. den Harder AM, Willemink MJ, de Ruiter QM, Schilham AM, Krestin GP, Leiner T, et al. Achievable dose reduction using iterative reconstruction for chest computed tomography: a systematic review. *Eur J Radiol* 2015; **84**: 2307–13. doi: https://doi.org/10.1016/j.ejrad.2015.07.011
25. Mello-Amoedo CD, Martins AN, Tachibana A, Pinho DF, Baroni RH. Comparison of radiation dose and image quality of abdominopelvic CT using iterative (AIDR 3D) and conventional reconstructions. *AJR Am J Roentgenol* 2018; **210**: 127–33. doi: https://doi.org/10.2214/AJR.17.18025
26. Sabel BO, Buric K, Karara N, Thierfelder KM, Dinkel J, Sommer WH, et al. High-Pitch CT pulmonary angiography in third generation dual-source CT: image quality in an unselected patient population. *PLoS One* 2016; **11**: e0146949. doi: https://doi.org/10.1371/journal.pone.0146949
27. Liang T, McLaughlin P, Arepalli CD, Louis LJ, Bilawich AM, Mayo J, et al. Dual-source CT in blunt trauma patients: elimination of diaphragmatic motion using high-pitch spiral technique. *Emerg Radiol* 2016; **23**: 127–32. doi: https://doi.org/10.1007/s10140-015-1365-y
28. Kim SH, Choi YH, Cho HH, Lee SM, Shin SM, Cheon JE, et al. Comparison of image quality and radiation dose between high-pitch mode and low-pitch mode spiral chest CT in small uncooperative children: the effect of respiratory rate. *Eur Radiol* 2016; **26**: 1149–58. doi: https://doi.org/10.1007/s00330-015-3930-x
29. Tacelli N, Darchis C, Pontana F, Faivre JB, Deken V, Duhamel A, et al. High-pitch, dual-source chest computed tomography angiography without electrocardiographic synchronization: evaluation of cardiac motion artifacts on pulmonary circulation. *J Thorac Imaging* 2013; **28**: 376–82. doi: https://doi.org/10.1097/RTI.0b013e31828d4209
30. Baumueller S, Alkadhi H, Stolzmann P, Frauenfelder T, Goetti R, Schertler T, et al. Computed tomography of the lung in the high-pitch mode: is breath holding still required? *Invest Radiol* 2011; **46**: 240–5. doi: https://doi.org/10.1097/RLI.0b013e3181feee1a
31. Prakash P, Kalra MK, Kambadakone AK, Pien H, Hsieh J, Blake MA, et al. Reducing abdominal CT radiation dose with adaptive statistical iterative reconstruction technique. *Invest Radiol* 2010; **45**: 202–10. doi: https://doi.org/10.1097/RLI.ob013e3181dzfeec